

tude for the second harmonic could easily be overlooked, but one should be able to separate the two sinusoids from accurate data, and thus determine q from Eq. (29). Unfortunately, the data referred to above^{3,4} were not satisfactory for this type examination because the oscillations has to be removed from the gross effect by graphical means. However, the use of a differential technique in recording the data plus the use of computer curve-fitting techniques should allow one to separate the first two harmonics. The relative amplitude B_2/B_1 is twice as large as A_2/A_1 so that the effect may be more easily observed in thermal phenomena. It is

clearly very important to be aware of the harmonic content of the oscillations due to a specific portion of the Fermi surface, especially when more than one piece of the Fermi surface may be contributing to the phenomena.

ACKNOWLEDGMENTS

We are indebted to Dr. C. G. Grenier for helpful discussions and suggestions. We also wish to thank Dr. W. D. Deering, Dr. M. E. Anderson, and Dr. L. F. Connell for valuable comments and critical reading of the manuscript.

Effects of Various Doping Treatments upon the Damage Production and Recovery of Deuteron-Irradiated Aluminum*

K. HERSCHBACH

Douglas Aircraft Company, Incorporated, Santa Monica, California

AND

J. J. JACKSON

Argonne National Laboratory, Argonne, Illinois

(Received 26 September 1966)

The effects of various doping treatments (cold work, alloying, and/or radiation doping) upon the damage production and recovery of Al irradiated with 20-MeV deuterons have been investigated. Four of a total of six specimens (two made from Al-0.03 at. % Zn alloy, one annealed, and one cold-worked) were irradiated with 10-MeV protons to a total dose of 3.3×10^{16} p/cm² at a temperature of about 90°K and annealed for 10 min at 180°K. These four radiation-doped and two additional specimens (one annealed and one cold-worked) were then irradiated simultaneously at a temperature not exceeding 8°K with 20-MeV deuterons to a total integrated dose of 4.85×10^{15} d/cm². Isochronal annealing measurements were carried out *in situ* up to 265°K. Within our accuracy ($\pm 10\%$), the damage production in all six specimens was the same; however, previous experiments indicate a small increase in damage production for doped specimens. No radiation annealing was found in the annealed 99.9999% Al, while a large effect was found in the cold-worked 99.9999% Al. Radiation doping produces the radiation-annealing effect in an annealed sample as well as in the alloy, and reduces the effect of cold working. Cold work and alloying reduce the recovery in stage I; radiation doping increases it. The annealing curves for alloys are smoothed out in stage II. Cold work and/or radiation doping do not affect stage II significantly, and all remaining damage anneals out in stage III. Because all six specimens underwent exactly the same thermal history, the difference in annealing, i.e., the percentage of damage left in specimen *A* minus the percentage of damage left in specimen *B*, was calculated for different specimen combinations and plotted. These curves reveal many small details in the different annealing behavior which have not been observed previously and which are caused by the different treatments prior to the irradiation. They are discussed in terms of interstitial migration in stage I. Specifically, it is claimed that the crowdion migrates at a temperature of about 45°K and that stage III is composed of (at least) three different annealing processes.

I. INTRODUCTION

RECENTLY, more and more attention has been paid to the study of radiation damage in metals other than copper, the metal most thoroughly investigated both theoretically and experimentally. This interest has been prompted by failure to develop an acceptable model for radiation damage, and by the fact that the extent to which radiation damage in

different metals is similar is not well understood. The main difficulty associated with radiation damage is centered around the so-called "stage-III dilemma," in which apparently more annealing stages are observed than there are point defects available. A study of the most current literature reveals that the disagreement in how to account for the recovery in stage III has become worse despite an ever increasing number of experimental investigations. The reason for this dilemma is obvious: Microscopic events must be inferred indirectly from the macroscopic properties used

* Supported by the Douglas Independent Research and Development (IRAD) program and by the U. S. Atomic Energy Commission.

to establish the damage (most commonly, electrical resistivity). Therefore, only by changing the conditions of the experiments in a controlled way can one obtain a sufficient amount of data, which then can be used to formulate a consistent explanation for the phenomena observed. This can be done, for example, by using different bombarding particles (different energy of the knockon atom), different damage concentrations (kinetic studies) and by doping, i.e., cold work, quenching, alloying, and/or radiation doping. Doping affects both the damage production (defocusing, dechanneling) and the recovery (trapping) and is the method most often applied in our radiation-damage experiments.

In two previous papers,^{1,2} we discussed the effects of various pre-irradiation treatments on radiation annealing and thermal annealing in aluminum, gold and platinum specimens in terms of the interactions of long-range transport events with lattice defects. It was proposed that damage enhancement in quenched platinum is caused by the deflections of dynamic crowdions by atoms relaxed toward single vacancies. Only selected pre-irradiation treatments were employed in the experiments because, unfortunately, we could not usefully employ prequenched aluminum and gold samples in our apparatus. Since we could not quench *in situ*, the quenched specimens remained at room temperature long enough during the mounting to allow annealing of the quenched-in vacancies. Therefore, for the experiment described in *this* paper, we used a somewhat different approach to introduce an excess of vacancies in aluminum. The specimens were irradiated below 95°K with 10-MeV protons which introduced point defects. The low-temperature stages I and II were eliminated by annealing up to 180°K prior to a second irradiation with 20-MeV deuterons.

The objective of the experiment described in this paper was to study closely the effects of cold working, alloying, and/or radiation doping upon the damage production and annealing of deuteron-irradiated aluminum in order to understand better what annealing processes were responsible for stages I through III. For this purpose, a novel approach was used. Since on our holder³ six specimens can be mounted simultaneously, they can be subjected to exactly the same annealing treatment after irradiation. Therefore, the difference in annealing for different specimen combinations, i.e., the percentage of damage left in specimen *A* less the percentage of damage left in specimen *B*, can be calculated with high accuracy. Differences in annealing as small as 0.1% of the total damage can be established. This high resolution, previously unattainable, has enabled us to obtain a wealth of data which are presented in Sec. III of this paper. As will be shown in Sec. IV, the results can best be discussed in terms

of interstitial migration in stage I. Stage III still poses a puzzle since our results indicate that at least *three* distinct processes are responsible for the annealing in stage III. The experimental procedures are briefly discussed in Sec. II.

II. EXPERIMENTAL

The irradiations were carried out with the 60-in. cyclotron at the Argonne National Laboratory. The cryostat and auxiliary equipment have been described previously.¹⁻³ A different aperture window was employed on which a springloaded shield held in place by a solenoid-actuated lever protected the specimens in positions No. 1 and No. 4 during the irradiation with protons. The specimens in the other four positions were irradiated with 10-MeV protons to a total integrated dose of approximately 3.3×10^{16} *p*/cm² at a temperature not exceeding 95°K. After this irradiation, they were annealed for 10 min at 180°K. All six specimens were then irradiated with 20-MeV deuterons to a total integrated dose of 4.85×10^{15} *d*/cm² at a temperature not exceeding 8°K. After the irradiation, the specimens were pulse annealed for 10 min in steps of 1°K up to 50°K, 5°K from 50 to 105°K, and in 10°K steps from 165 to 265°K. The amount of damage was established by resistance measurements; the precision of these measurements was, for all specimens, better than 0.1% of the total resistivity increase due to the deuteron bombardment.

The specimens were prepared in the same way as described in Ref. 1. Two each of 99.9999% annealed Al (positions 1 and 3), Al-0.03 at% Zn (positions 2 and 5), and 99.999% cold-work Al (positions 4 and 6) were mounted. The pertinent irradiation data for the specimens are given in Table I. One of our alloyed specimens was annealed in air; the other probably had been annealed in an inert atmosphere. They seem to be different, as one can see from the resistance ratio $R_{300^\circ\text{K}}/R_{4^\circ\text{K}}$, which was 63 for specimen No. 2, and 145 for specimen No. 5. The latter ratio corresponds to the ratios previously found for specimens annealed in an inert gas atmosphere. Therefore, it might be possible that we unintentionally mounted two alloyed specimens with different annealing history. The specimens showed small, but real differences in the annealing (see below). As mentioned above, specimens No. 1 and No. 4 were not irradiated with protons.

We experienced some technical difficulties with specimen No. 1. After the 125°K anneal, the specimen was apparently in poor electrical contact with the clamps which hold the specimen in place, so that no annealing data could be obtained for the annealed 99.9999% Al above 125°K. The resistivity increases due to cold work in specimens Nos. 3 and No. 6 were of the order of 1.2×10^{-8} Ω-cm. This is about half of the increase in one of our previous experiments (Refs.

¹ K. Herschbach and J. J. Jackson, Phys. Rev. **153**, 689 (1967).

² J. J. Jackson and K. Herschbach, Phys. Rev. **153**, 694 (1967).

³ K. Herschbach, Rev. Sci. Instr. **37**, 171 (1966).

TABLE I. Resistivity increments^a (Ω -cm).

Specimen history	No. 1 99.9999% Al annealed	No. 2 Al-0.03 at.% Zn annealed radiation doped	No. 3 99.9999% Al annealed radiation doped	No. 4 99.9999% Al cold-worked	No. 5 Same as No. 2	No. 6 99.9999% Al cold-worked radiation-doped
95°K		8.08×10^{-9}	7.22×10^{-9}		6.97×10^{-9}	9.79×10^{-9}
After anneal at 180°K		4.97×10^{-9}	4.12×10^{-9}		3.83×10^{-9}	5.57×10^{-9}
Deuteron irradiation	5.28×10^{-9}	5.25×10^{-9}	5.26×10^{-9}	5.64×10^{-9}	5.66×10^{-9}	5.57×10^{-9}

^a About 10% of the specimen length was not irradiated. The data are not corrected for this fact.

1 and 2—Caltech specimen), and corresponds to a dislocation density of 1×10^{11} cm/cm³.⁴

III. RESULTS

A. Damage Production and Radiation Annealing

Because of the difficulties involved in shaping the beam and irradiating an exactly measured length of the specimen, our production rates may be in error by as much as 10%, even though the precision is much better. Within these limits of error, the *total damage production* at the end of the run (integrated flux 4.85×10^{15} d/cm²) was the same in all six specimens. (Because of radiation annealing the production *rate* is dose-dependent.)

If we accept the data at face value, then at the end of the run the *production rate* with respect to specimen No. 1 (99.9999% Al, annealed, hereafter, called the standard specimen) was higher by 7% in specimen No. 5 (Al-0.03 at% Zn), higher by 3% in specimen No. 4 (99.9999% Al, cold-worked), and higher by 4% in specimen No. 6 (99.9999% Al, cold-worked, radiation-doped). Specimens No. 2 (Al-0.03 at% Zn) and No. 3 (99.9999% Al, radiation-doped) had the same production rate as the standard.

The decrease in the production rate with flux (radiation annealing) can, however, be established with more accuracy since neither the geometry of the apparatus nor, hopefully, the beam shape change during an experiment. In Fig. 1 the production rates have been plotted against integrated flux. No effort has been made to fit a particular curve through the points. The general trend can be easily seen, and is in agreement with our prior findings.¹ No radiation annealing was found in the 99.9999% annealed Al, and a large effect in the cold-worked specimen was reduced by radiation doping. Radiation annealing is observed in annealed, radiation-doped Al as it was observed in quenched Pt, which also contained an abundance of vacancies.¹ The alloyed specimens, both of which were radiation doped, showed a small radiation-annealing effect. Unfortunately, we do not have very reliable results on this effect in annealed, alloyed specimens.

In summary, we can say that radiation doping

⁴ T. Federighi, S. Ceresara, and C. Panseri, *Nuovo Cimento* **29**, 1223 (1963).

produces radiation annealing in annealed Al specimens and reduces the effect in cold-worked ones. If there is an increase in the production rate due to any of the treatments, it is small, in agreement with previous findings.¹

B. Isochronal Annealing Studies

Figure 2 shows the result of the isochronal annealing studies for all six specimens. The apparent negative annealing is the result of the radiation doping, since above 180°K the damage introduced by the proton bombardment and still left in the specimens anneals out simultaneously with the damage introduced by the deuteron irradiation. The curves show the familiar features of suppression of stage I by cold work,² and by alloying,^{2,5-7} but also show that radiation doping increases stage I except in the alloy. The latter fact can be arrived at only indirectly by comparison with our previous experiments.^{1,2} At 50°K, the suppression in the same alloy was 10% in Argonne run No. 2 and in the Caltech run, versus 9% in this experiment. The enhancement of stage I is approximately the same percentage wise for both annealed and cold-worked specimens (see below for more details). Radiation dop-

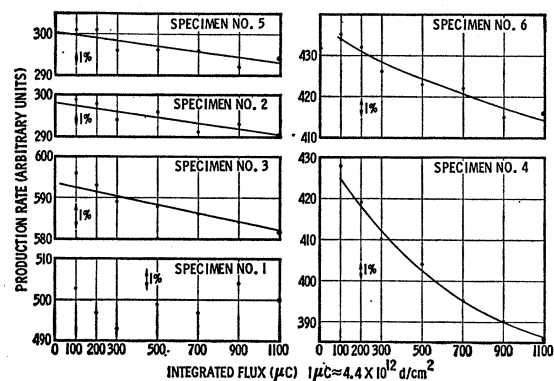


Fig. 1. The damage production rates for all six aluminum specimens have been plotted against integrated deuteron flux. Deuteron energy was 20-MeV. The 1% bars have been added to help visualize the magnitude of the radiation annealing effect. The specimen history is described in the text and in Table I.

⁵ A. Sosin and L. H. Rachal, *Phys. Rev.* **130**, 2238 (1963).

⁶ C. L. Snead, Jr. and P. E. Shearin, *Phys. Rev.* **140**, A1781 (1965).

⁷ M. L. Swanson and C. R. Piercy, *Can. J. Phys.* **42**, 1605 (1964).

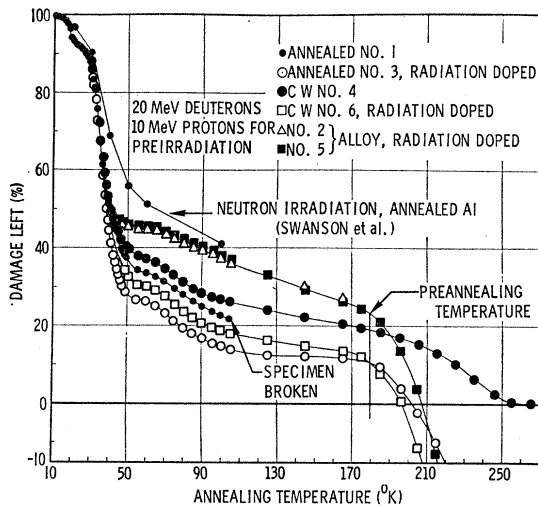


FIG. 2. Isochronal annealing curves for 10-min annealing at each temperature. The apparent negative annealing is caused by the radiation doping.

ing, therefore, has the same enhancing effect as quenching on neutron-irradiated Al.⁷

Another noteworthy feature is the difference in annealing between the alloys and any of the other pure specimens in the temperature range 60–170°K. (Once again, strictly speaking, we can say this only for radiation-doped alloys, but a comparison with previous results² shows quickly that the alloys anneal in an identical manner whether or not they are radiation-doped. Therefore, no further distinction will be made throughout this paper between alloyed specimens which were radiation-doped and alloys which were not.) While the pure samples show a distinct annealing peak near 80°K, and anneal much less at higher temperatures, the annealing curve for the alloys is almost a straight line from 60 to 170°K. This is in marked contrast to the findings by Sosin *et al.*⁵ who, despite bigger temperature steps than those employed in the present investigation (25 versus 20°K) observed a distinct annealing peak in Al–0.1 at% Zn after irradiation with 1-MeV electrons. The peak was situated

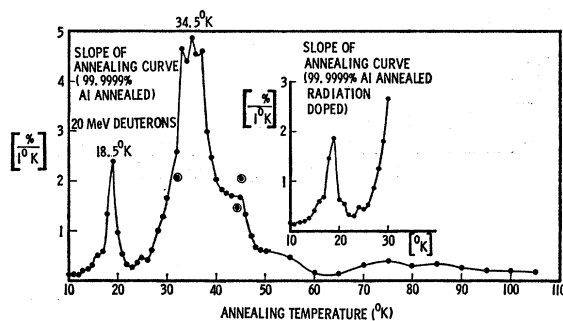


FIG. 3. Slope of the isochronal annealing curves for 99.9999% annealed Al and 99.9999% annealed, radiation-doped Al (insert).

between 125 and 150°K, and accounted for about 8% annealing. There was practically no annealing in their specimen between 150 and 175°K (see Figs. 2 and 9 in Ref. 5). They also had suppression of annealing at around 20°K, which is also contrary to our findings (see below). The results found by Snead *et al.*⁶ after 2-MeV electron irradiations of their alloys were similar to the results of Sosin *et al.*,⁵ except that in their Al–0.3 at% Zn more than 10% of the damage annealed out between 125 and 150°K. On the other hand, the data from the neutron irradiation experiments by Federighi *et al.*⁸ support our findings, except that they found some small structure in the annealing curve of their Al–0.1 at% Zn alloy. They used temperature steps of 10°K, so this structure might have escaped our detection. If one extrapolates to the total damage which would have been introduced had the irradiation been carried out at a temperature below 10°K, one gets an annealing of 3% between 125 and 150°K. This compares with 4% in the deuteron case. However, Federighi *et al.*⁸ used a total damage an order of magnitude larger than employed in the other experiments discussed here. It seems that in our Zn alloy, whatever annealing processes going on in stage II (60–180°K) are spread over the whole temperature range after heavy particle bombardment. This spread can be observed to some extent in our cold-worked specimens, which were fabricated from somewhat less pure aluminum than that used for the annealed specimens. It is therefore clear that stage II is very much affected by impurities and by the kind of particles used, but is not affected to a great extent by radiation doping.

The derivative of the isochronal annealing curve for the standard specimen is given in Fig. 3 and shows the details known from previous investigations on aluminum with deuterons⁹ as well as with electrons,^{6,10–13} A large peak, split into at least three subpeaks, is centered at 35°K, and a distinct narrow peak is located at 19°K. A third large peak appears as a shoulder on the high-temperature side of the largest peak at about 45°K. A number of small peaks are located at 13.5, 16.5, 25, and 55°K, and two more peaks are apparent between 70 and 90°K. Some additional peaks seem to be hidden on the low-temperature side of the 35°K peak.

C. Comparison of Annealing Data

As already mentioned, a thorough comparison of the annealing of differently treated specimens was the main

⁸ T. Federighi, S. Cersara, and F. Pieragostini, *Phys. Letters* **6**, 152 (1963).

⁹ K. Herschbach, *Phys. Rev.* **130**, 554 (1963).

¹⁰ W. Bauer, J. W. Deford, J. W. Kauffman, and J. J. Koehler, *Phys. Rev.* **128**, 1947 (1962).

¹¹ K. R. Garr and A. Sosin, *Bull. Am. Phys. Soc.* **10**, 1179 (1965).

¹² H. I. Dawson, G. W. Iseler, A. S. Mehner, and J. W. Kauffman, *Phys. Letters* **18**, 247 (1965).

¹³ H. I. Dawson, G. W. Iseler, and J. W. Kauffman, in *Lattice Defects and Their Interactions* edited by K. K. Hasiguti (Gordon and Breach Science Publishers, Inc., New York, to be published).

objective of this investigation. For each specimen, the remaining damage percentage was calculated after annealing step and compared with the damage for a "reference" specimen. This reference specimen can be any of the six specimens depending on what effect we want to study. Because of the identical thermal history, the difference in percentage represents exactly the "deviation" of the particular specimen from the reference specimen. This difference has the big advantage of being unaffected by unavoidable heating errors.

In Fig. 4 the usefulness of this approach becomes immediately apparent. Specimen No. 1 (99.9999% Al, annealed) was chosen as reference. The curves show a great many details reflecting the influence of the different treatments prior to the deuteron bombardment. The general trend is quite obvious, namely, suppression

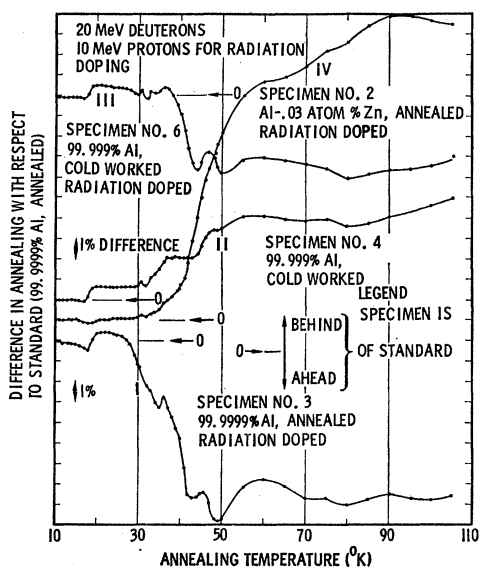


FIG. 4. The difference in annealing, i.e., the percentage of damage left in a specimen minus the percentage of damage left in the 99.9999%, annealed specimen has been plotted against annealing temperature. Zero difference has been indicated for each curve.

of stage I by alloying and cold work, and enhancement of stage I (except for the alloy, see above) by radiation doping. It is also obvious that these simple statements do not cover all the effects observed. To further emphasize the different effects caused by the different treatments, other specimen combinations have been plotted in Fig. 5. Finally, in Fig. 6, the difference for an annealed versus a cold-worked specimen from an earlier experiment has been plotted. The amount of cold work retained was twice as much as in the present experiment, and the total damage was about 1.6 times larger than in the present experiment. For easy reference the curves in Figs. 4-6 have been numbered consecutively I-VIII. The observations are best discussed according to the temperature intervals in which they occur.

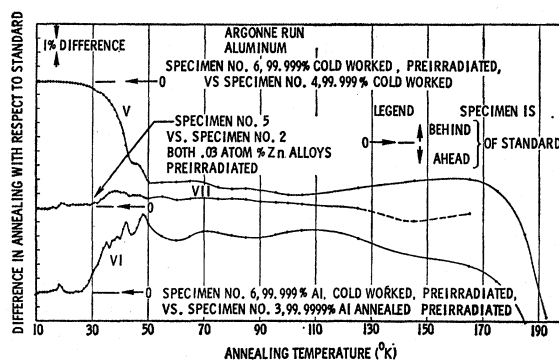


FIG. 5. Same as in Fig. 4, except that specimens have been compared as indicated.

1. The Low-Temperature Region ($T \leq 20^\circ\text{K}$)

At about 18-19°K the annealing in all but the alloyed specimens starts to fall behind normal annealing (I, II, III, and IV). The suppression of annealing is caused by radiation doping of annealed Al (I) and by cold work (II, III), but is not further increased by radiation doping of a cold-worked specimen as can be seen from curve V, where a cold-worked, radiation-doped sample is compared with a specimen which was cold worked only. The total amount of suppression depends on the total dose and/or the amount of cold work retained in the sample.

From an earlier experiment (reported in Refs. 1 and 2), we conclude that the amount of cold work is the more important of the two factors involved. In curve VIII, the suppression at 18°K is twice as much as in the present experiment, as was the amount of cold work, while the total damage was about a factor 1.6 higher. On the other hand, in Argonne run No. 4, reported in the same paper,^{1,2} very little cold work was left in the cold-worked sample as measured by the resistivity prior to the irradiation. During the bombardment, this specimen exhibited radiation annealing typical of a cold-worked specimen, but it annealed without showing

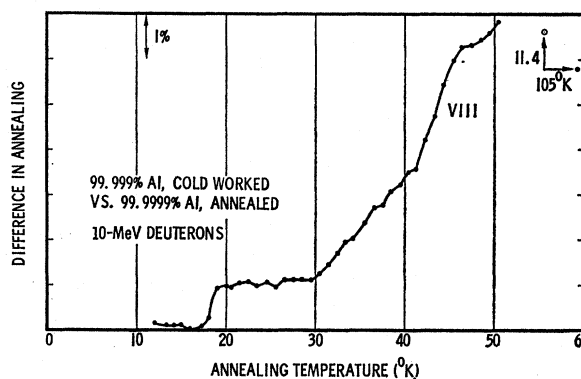


FIG. 6. Same as in Fig. 4 for specimens from an earlier experiment (Ref. 2). The value measured for the highest annealing temperature has been indicated in the upper right-hand corner. For more details see text.

suppression of recovery in stage I, even though the total damage was almost four times larger than in the present experiment.

In the 99.9999% Al specimen which was radiation doped, the suppression at 18°K is preceded by faster annealing at around 16°K (I). This faster annealing is the reason for the little peak at 16°K in curve VI. What has happened can best be seen from the slope of the annealing curve, plotted as an insert in Fig. 3. The little peak at 16.5°K is enhanced, while the 18.5°K peak is suppressed. There is no such little peak in curve V which compares the two cold-worked specimens. This proves that the effect just discussed can be produced only in radiation-doped, annealed Al. Whether or not enhancement and suppression cancel each other above 20°K, as they do in the present experiment (e.g., see curve VI), or whether that depends on the amount of radiation doping, cannot be decided from our data.

2. 20–30°K Interval

Although there is appreciable annealing in the temperature range 20–30°K (Figs. 2 and 3), the different doping treatments seem not to have any effect in this temperature interval except for the 99.9999% annealed, radiation-doped Al, in which annealing goes faster than in the reference specimen starting from about 27°K.

3. The 30–50°K Interval

While the suppression in annealing discussed above was associated with the first distinct annealing peak at 19°K, greater differences in annealing show up in the temperature range of the large peak centered at 35°K and its associated peak at 45°K. For the cold-worked specimen the main suppression occurs in two separate steps, one centered at 35°K and the other one at 45°K (II). For the other specimens, the effects are more or less spread out over the 30–50°K temperature range. Nevertheless, this range probably consists of two overlapping temperature regions, one approximately covering the annealing from 30–40°K, the other from 40–50°K. Both will therefore be discussed together. The most important features in both regions are described below.

(a) The annealing in the radiation-doped, annealed 99.9999% Al specimen is greatly enhanced [I]; however, near 36°K there is a small suppression, beyond which the enhancement is even more pronounced at about 40°K. There is some more suppression in the range 40–50°K. This latter effect is very pronounced for the cold-worked, radiation-doped sample (III).

(b) In the cold-worked, radiation-doped specimen the enhancement in annealing is centered more toward 40°K and starts only at about 37°K (III), which is 10°K higher than in the annealed, radiation-doped sample.

(c) Radiation doping apparently does not alleviate the suppression of stage I in the alloyed samples. Suppression starts at 35°K, and becomes rapidly larger about 40°K (IV).

(d) The steps in the curve for cold-worked aluminum (II), were mentioned above. In curve VIII, these steps are reduced in shape to merely two different slopes of the curve, but in that experiment the cold-work retained in the specimen was twice as large, and the damage larger by a factor 1.6 than in the present experiment. (Apparently, the second step, centered at about 45°K has been moved toward lower temperature!) Even on the curves for the radiation-doped alloy, the different slopes can be determined.

However, the "45°K" slope seems to be better described as consisting of two different slopes with the break occurring at 45°K. This "break" corresponds to the dimple in the curves for the radiation-doped, cold-worked (III) and radiation-doped, annealed (I) Al, being larger for the cold-worked one. It can also be seen from curve VI (take the mirror curve). But the effect is very small when cold-worked specimens are compared (V). We therefore can conclude that this suppression is (mostly?) due to the cold work, but can be overcome by radiation doping.

(e) In this connection it is interesting to note that despite both cold-worked specimens having had almost the same amount of cold work and having been irradiated to the same integrated flux, curves I and II do not add up to curve III, as they should if the effects of cold work and radiation doping were additive.

(f) When cold-worked specimens, one of which was radiation doped, are compared, a remarkably smooth curve results (V), except for a little dimple already discussed above. Radiation doping apparently enhances the annealing very gradually without relation to the many discrete annealing peaks. It is also significant that this enhancement does not affect stage II. Both specimens anneal in parallel curves.

4. Stage II

Above 50°K only alloying has any significant effect upon the annealing (curve IV). Up to about 90°K, the annealing is still suppressed in the alloys. Starting at 55°K, the slope of curve IV changes again, indicating that possibly another process is taking over. There is also indication of a similar process (trapping?) at 60°K in the annealing of the annealed, radiation-doped Al specimen.

Because our reference specimen broke after the 105°K anneal, we can only indirectly deduce what effect radiation doping has through stage III. As one can see from curves V and VII, the effect is apparently negligible. There is a slight difference in the annealing behavior of the two alloyed, radiation-doped samples (VII). We do not have sufficient information to determine the reason for this discrepancy.

D. Stage III

Though we unfortunately lost the reference specimen at 105°K, we have nevertheless plotted in Fig. 7 the slope of the annealing curve for four specimens in the stage III annealing region. The ordinate is given in arbitrary units. (Actually, the ordinate is given in $\Omega\text{-cm}/^\circ\text{K}$ times a factor common to all specimens, so numbers for the four specimens may be directly compared.) Only one specimen (No. 4, cold-worked Al) was not radiation doped, so it shows much smaller stage-III annealing with the main peak centered at around 240°K. The most noteworthy feature is the shift of the (same?) peak for the other three specimens. This shift, however, does not show a simple relation to the absolute concentration. Apparently the peak is centered at the lowest temperature for the radiation-doped alloy (225°K) and at the highest temperature for the radiation-doped annealed 99.9999% Al, where the peak occurs at a higher temperature than in the cold-worked specimen, even though the absolute damage in the latter is five times smaller. The curve for the radiation-doped, annealed Al shows in addition a satellite peak at 225°K and a smaller one at 195°K. The latter peak is also present to some degree in the other specimens.

IV. DISCUSSION

We propose to discuss our results within the framework of the two-interstitial model since we think

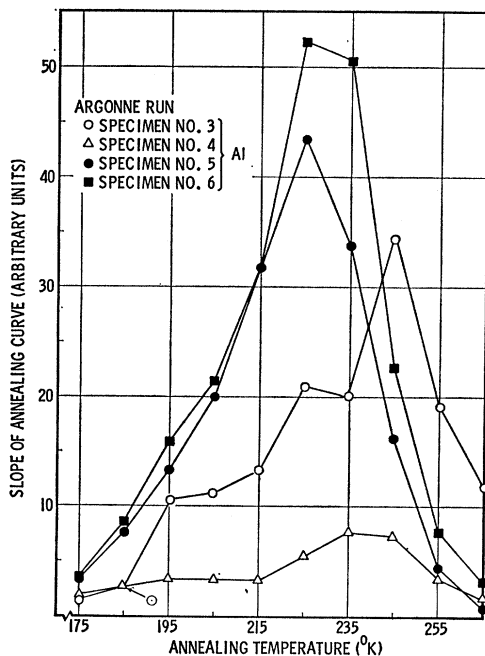


Fig. 7. Slope of the annealing curves through stage III. The ordinate is given in arbitrary units as explained in the text.

(despite objections from some authors)^{14,15} that this model can best account for the experimental observations. The two-interstitial model was first applied to aluminum by Sosin *et al.*⁵ and later, again to electron-irradiated Al, by Snead *et al.*⁶ Basically, this model postulates that two stable interstitials are produced upon irradiation. One gives rise to the annealing at the end of stage I and is commonly believed to be the (110) interstitial (crowdion). The other one migrates in stage III and is supposed to have the (100) configuration (split-interstitial).^{5,6} The low-temperature parts of stage I and stage II are caused respectively by the annihilation of close Frenkel pairs and by the release of crowdions from traps. In the case of aluminum there is additional evidence for the migration in stage III of a point defect with tetragonal symmetry, most likely the split-interstitial.¹⁶

A somewhat modified two-interstitial model has been proposed by Federighi *et al.*¹⁴ who assign the second interstitial to stage II with the vacancy moving in stage III.

On the other hand, the interstitial-vacancy model assumes that only one interstitial is stable and moves in stage I. Stage III is produced by vacancy migration. While the interstitial-vacancy model accounts for the stage-I suppression in alloys in the same way as the two-interstitial model does, namely, by assuming that the freely migrating interstitial is trapped by the impurities, it cannot account satisfactorily for the suppression of stage I in cold-worked specimens. This is the main reason that we prefer the two-interstitial model, which, however, is not free of difficulties either: Federighi *et al.*,¹⁴ found the activation energy for stage III in *neutron-irradiated* aluminum to be the same as that for the recovery of quenched aluminum and therefore attributed stage III to vacancy migration. Our annealing curves (Fig. 7) indicate that more than one process is going on in stage III and there might be room for both interstitial and vacancy migration in what is grouped together in stage III.

Let us try to account for our observations within the framework of the two-interstitial model. Most close Frenkel pairs should not be affected by impurities, so the peak at 18.5°K (Fig. 3) is not suppressed by alloying. This is in disagreement with the results by Snead *et al.*,⁶ who observed this peak after electron bombardment at exactly the same temperature, but found suppression in the three alloys investigated (see Table II in Ref. 6).

Suppression of the 18.5°K peak was also found by Sosin *et al.*⁵ Why was suppression found in the case of electron irradiation? First of all, the concentrations of the impurities were much higher than in our speci-

¹⁴ T. Federighi, S. Ceresara, and F. Pieragostini, *Phil. Mag.* **12**, 1093 (1965).

¹⁵ K. Ono, M. Meshii, and J. W. Kauffman, *Acta Met.* **12**, 391 (1964).

¹⁶ D. Keefer and A. Sosin, *Acta Met.* **12**, 969 (1964).

mens (more than a factor of 3 for the alloys employed by Sosin *et al.*,⁵ and a factor of 10 in the case of Snead *et al.*⁶). Certainly, one can increase the impurity content to a point where even close Frenkel pairs will be affected. In the alloys employed by Snead *et al.*, for instance, the mean separation of impurity atoms (assuming random distribution of course) was only about *seven* lattice spacings, and in the alloy employed by Sosin *et al.*, *ten* lattice spacings. The mean distance between Zn atoms in our alloy was about *fourteen* lattice sites. This argument is further supported by the amount of suppression, which was 7% in the case of Snead *et al.* compared to 4% found by Sosin *et al.*, and 0% for our 0.03 at% alloy.

That the history of alloyed specimens plays a role can be seen from our own experiments (curve VII). Even though the two specimens were prepared from the same material, they show small differences in the annealing behavior. These facts then could account for the different amounts of suppression found in the various peaks in stage I.⁶

Suppression in our alloyed specimens does not start until about 32°K and seems to come about in more or less discrete steps, as can be seen from Fig. 4. Beyond the temperature region of the large peak at 35°K, suppression is relatively slow up to 40°K. After that, however, the alloyed specimens fall rapidly behind the standard up to about 50–55°K, a temperature interval in which very little annealing is going on in electron-irradiated aluminum (even in high-purity samples), but in which the annealing in deuteron-irradiated Al is still large (Fig. 2). Snead *et al.*⁶ ascribe the 35°K peak to the freely migrating crowdion. We think, however, that this opinion has to be viewed with some reservation. First of all, we do not find—within the errors of this and Snead's investigation—a temperature shift for the 35°K peak. Assuming second-order kinetics and taking an activation energy of 0.11 eV,⁹ the temperature shift should be about 1°K.¹⁷ We also do not find a peak shift in an earlier experiment (Ref. 2, Caltech run) for which the annealing curve has been plotted in Fig. 8. Secondly,

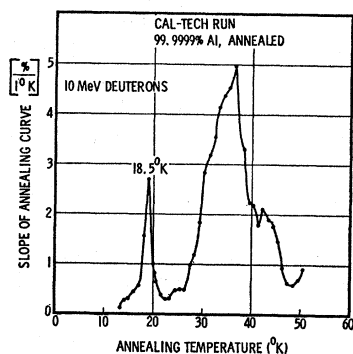


FIG. 8. Slope of the annealing curve for 99.9999% annealed Al, irradiated with 10-MeV deuterons (data taken from experiment described in Ref. 2).

this interpretation would preclude an explanation of the other peaks in the large peak about 35°K. Certainly, the energy necessary to form these defects is not much different from the formation energy for the crowdion; nevertheless, the extra structure is only seen after heavy charged particle bombardment. A more logical explanation would be that up to 45°K these peaks are all due to close Frenkel pairs, some of which are formed only when the displaced atom receives much energy. The higher energy is required not so much to *form* these pairs as to achieve a specific form of propagation of the primary (focusing or channeling). This would also explain the different shapes of the large peak found after irradiation with different deuteron energies (Figs. 3 and 7). The width and substructure of the peak also support this view. Finally, there is indication that the peak found in our investigation at 45°K is shifted toward lower temperature with higher damage rate, indicating that the underlying process is of an order different from unity. This shift can be seen by comparing Figs. 3 and 8. (Theoretically,¹⁷ this shift should have been 1.9°K assuming second-order kinetics and taking a migration energy of 0.14-eV⁹.)

The peak would correspond to the very small one found at 50°K in *pure* Al by Snead *et al.*⁶ It was indeed completely suppressed in the Zn and Cu alloys, as it should be if the peak is caused by *freely* migrating interstitials facing an abundance of traps.

We therefore tentatively propose to assign the 45°K peak to the freely migrating interstitial which is in all probability the crowdion. This view is further supported by the results of internal friction measurements on electron-irradiated Al,¹⁸ which show that defects begin to migrate to dislocations and pin them at about 40°K. The suppression then of the 35°K peak in our alloys is due to long-range interaction between the impurity atoms and the (close) Frenkel pairs. The concentration of the impurity atoms is high enough to affect the more widely separated interstitial-vacancy pairs, but not the ones which are closer to each other.

Let us consider the influence of cold work. Dopants can react both dynamically and statically with crowdions. Apparently the dislocations change the damage production by converting the dynamic crowdion into a stable split interstitial.^{5,19} Therefore, there should be some suppression throughout *all* of stage I, and that is what we observe (Fig. 4, curve II and Fig. 6, curve VIII). All peaks are reduced in stage I, and there is no effect on stage II. The amount of suppression quite logically seems to depend on the amount of cold work² (Fig. 6, curve VIII). It is significant that suppression in the 45°K peak is as big as in the 35°K peak despite the fact that the total annealing is much less, probably even less than in the 18.5°K peak. This, however, is

¹⁸ D. Keefer (private communication).

¹⁷ G. Burger, H. Meissner, and W. Schilling, *Phys. Status Solidi* 4, 267 (1964).

¹⁹ C. J. Meechan, A. Sosin, and J. A. Brinkman, *Phys. Rev.* 120, 411 (1960).

in agreement with our assumptions, since one would expect to have relatively more dynamic crowdions converted into split-interstitials which would otherwise become *freely* migrating crowdions well separated from their original vacancy. They simply have to travel farther, and therefore have a greater chance to encounter a dislocation.

How then do effects caused by radiation doping fit into this picture? The extra sinks provided by the radiation doping (mostly single vacancies ($C_V \approx 2.5 \times 10^{-3}$ at%) should not affect close Frenkel pair annealing unless they are really abundant (see discussion above about impurities). This simple conclusion is basically confirmed by the experiment (Fig. 4, curve I). However, enhancement of annealing begins to take place in the temperature interval of the large peak. This again, we think, is a question of defect concentration.

Because of the large number of extra vacancies, some crowdions which would otherwise become annihilated only as freely migrating interstitials can now form close Frenkel pairs with the extra vacancies. Consequently, they anneal at lower temperatures.

The slowing down of the *enhancement* in annealing for both the annealed and the cold-worked, radiation-doped specimens at 45°K is probably due to the non-pre-irradiated specimen catching up; since the crowdion can now move freely the *extra* sinks are no longer required. Significantly, this effect is larger for the cold-worked, radiation-doped sample. It should be, if dislocations convert dynamic crowdions into split-interstitials which are immobile at this temperature. This can be taken as further support for the assignment of the 45°K peak to the freely migrating crowdion. It is interesting to note the difference in the annealing of prequenched⁷ and radiation-doped Al with respect to annealed Al, even though the former was irradiated with neutrons. Up to about 60°K the difference between the treated and the annealed samples is very nearly the same, but in the prequenched Al the annealing is still enhanced up to 100°K, the highest annealing temperature employed (in the neutron case).

This extra enhancement for the quenched Al falls within the stage II annealing interval where there is very little annealing in the electron-irradiated Al^{6,7} but still an appreciable amount of annealing in deuterium- and neutron-irradiated Al, at least in pure samples. In our case, as was already pointed out, the annealing in stage II is practically unaffected by any of the doping treatments except alloying. It seems that at least after heavy particle bombardment, i.e., when the primary knock-on receives a high energy, stage II is an intrinsic effect which can be *disturbed* by *high* impurity content.

The small peak at 16.5°K (Fig. 3), which was barely noticeable in the Caltech run (Fig. 8), seems to depend more on the deuteron energy than on the total damage, since it was also found in a previous experiment with

a higher total damage but the same deuteron energy [cf. Ref. 9: Fig. 9(c)]. This peak is enhanced noticeably by radiation doping for *pure*, annealed Al, but the 18.5°K peak is suppressed in the same sample. However, to a small degree, this enhancement is present in all radiation-doped specimens, as can be seen from Fig. 4. Since this peak was not found after electron irradiation,⁶ we conclude that channeling is important for the creation of this defect, and that the channeled atom is stopped close to an already present vacancy. Since channeling is disturbed by alloying and by cold work, these particular Frenkel pairs are created in lesser numbers in specimens thus treated.

The large suppression of the 18.5°K peak in the annealed, radiation-doped Al (the largest suppression of all specimens) is rather surprising, especially since it cannot be enhanced further by cold work (Fig. 4, curve III). Actually, it was even smaller in the cold-worked, radiation-doped specimen (0.9% suppression versus 0.6%). Suppression of the 18.5°K peak is proportional to the amount of cold work, as mentioned above. It is apparently related to the number of point defects trapped on the dislocations² and it seems that point defects are responsible for the suppression. Therefore, point defects introduced by radiation doping act the same. The reason that cold work does not increase the suppression is simply that point defects at the dislocations have been reduced in number by the radiation doping. The suppression at higher temperatures (above 30°K) is, however, a true dislocation effect, as indicated by the smaller enhancement in the cold-worked specimen (Fig. 4, curve III). The equivalence of point defects, whether created on dislocations or by radiation doping, is shown in Fig. 5, curve V. Radiation doping of previously cold-worked Al simply increases the number of sinks. These sinks work better the farther apart the interstitial-vacancy pair, and of course work best for freely migrating crowdions. Above the migration temperature for the latter, there is no longer any difference!

Regardless of whether stage III annealing in deuterium-irradiated Al is attributed to interstitial or vacancy migration, we are, at the moment, at a loss to explain the observed recovery (Fig. 7). In either case, one would expect radiation doping simply to increase stage III (with the appropriate peak shift toward lower temperature). However, the observed behavior is much more complex. Not only is the big peak shifted contrary to what one would expect from the different damage concentrations, but it becomes obvious that stage III consists of at least three different processes. This can be most clearly seen on the curve for the 99.9999%, annealed, and radiation-doped Al (specimen No. 3). The largest peak, centered at around 245°K, occurs at a temperature approximately 5°K *higher* than the similar peak in the 99.9999%, cold-worked Al, but the damage annealed out in stage III

is smaller by about a factor of 5. One possible explanation is that more than one point defect is responsible for stage III.

V. SUMMARY

The observations made in this investigation can best be interpreted within the framework of the two-interstitial model.

(1) Impurities trap the free migrating interstitial in stage I. With higher impurity concentrations, the interstitial in distant Frenkel pairs can also be trapped, resulting in suppression of *lower-temperature peaks* in stage I.

(2) Up to 45°K, all annealing peaks are due to close pair annealing. The population number of some peaks depends on the energy of the primary, not so much because of a high formation energy for this configuration as because a high energy is required to obtain a specific form of propagation of the primary (focusing, channeling).

(3) The peak found at 45°K in this experiment can best be attributed to the free migrating crowdion.

(4) Crowdions are converted at dislocations into split interstitials. Consequently, stage I is suppressed by cold work and stage III is enhanced. The amount of suppression depends on the amount of cold work and *all* peaks are reduced in stage I. The 45°K peak is reduced the most, as is to be expected, because the crowdions which normally would contribute to this

peak have the greatest chance to encounter a dislocation since they travel the farthest.

(5) Radiation doping enhances stage I by providing extra sinks in the form of vacancies. If crowdions are created close to extra vacancies, they form Frenkel pairs. Consequently, even annealing in close pair peaks is enhanced.

(6) Stage II is affected only by alloying, not by the other doping treatments. Therefore, stage II, at least after heavy charged particle bombardment, seems to be an intrinsic effect which can be disturbed by high impurity content.

(7) Stage defects introduced by radiation doping act the same as point defects trapped on dislocations.

(8) Stage III consists of at least three distinct annealing processes. It seems possible that more than one point defect might migrate in stage III; however, no definite conclusion could be drawn from the present data.

The stage III dilemma was not solved by the present investigation, even though some new insight was gained. Certainly, more work has to be done, and similar experiments on copper and silver are currently in progress.

ACKNOWLEDGMENTS

The authors wish to thank Ed Ryan for his patience in helping with the experiment, and M. Oselka and the cyclotron crew at the Argonne National Laboratory for performing the irradiations

Relationship between the "Proton-Proton" and "Proton-Electron" Dielectric Constants

L. E. BALLENTINE

Theoretical Physics Institute, University of Alberta, Edmonton, Alberta, Canada

(Received 30 January 1967)

In an interacting electron gas one may distinguish between the "proton-proton" dielectric constant, which is the ratio of the applied electric field to the resultant electric field, and the "proton-electron" dielectric constant, which is the ratio of the applied electric field to the resultant electric field plus effective exchange and correlation field as would be experienced by an electron. The relationship between these two quantities is derived and used to prove that two recently proposed expressions for the structure-dependent energy of a metal are identical.

CONSIDER a homogeneous interacting electron gas to which is applied an external sinusoidal electrostatic potential $V_{\text{ext}}(\mathbf{q})$ of wave vector \mathbf{q} . The linear response measured by an external test charge (not an electron) can be written as

$$V_{\text{ext}}(\mathbf{q}) + V_H(\mathbf{q}) = V_{\text{ext}}(\mathbf{q}) / \epsilon_1(q), \quad (1)$$

where V_H is the electrostatic potential set up by the induced electron distribution $\rho(\mathbf{q})$. Equation (1) defines

ϵ_1 which we will call the "proton-proton" dielectric screening function. It has been shown^{1,2} that the many-electron problem can, in principle, be reduced to a set of one-electron problems in which each electron experiences an effective potential

$$V = V_{\text{ext}} + V_H + V_{\text{ee}}. \quad (2)$$

¹ P. Hohenberg and W. Kohn, Phys. Rev. **136**, B864 (1964).

² W. Kohn and L. J. Sham, Phys. Rev. **140**, A1133 (1965).